Drug Design, Development and Therapy

Dovepress
open access to scientific and medical research

Open Access Full Text Article

ORIGINAL RESEARCH

Metabolomics Combined with Network Pharmacology-Based Strategy to Reveal the Underlying Mechanism of Zhenhuang Submicron Emulsion in Treating Oropharyngeal Mucositis Complications of Radiation Therapy for Head and Neck Cancer

Wei Chen[1,*], Chunyu Li[1,*], Dujia Jin[2], Yafei Shi[1], Mingyu Zhang[1], Mingming Bo[1], Di Qian[1], Mengyang Wang[1], Guohui Li[1]

[1]Department of Pharmacy, National Cancer Center/National Clinical Research Center for Cancer/Cancer Hospital, Chinese Academy of Medical Sciences and Peking Union Medical College, Beijing, People's Republic of China; [2]Institute of Materia Medica, Chinese Academy of Medical Sciences and Peking Union Medical College, Beijing, People's Republic of China

*These authors contributed equally to this work

Correspondence: Guohui Li, Department of Pharmacy, National Cancer Center/National Clinical Research Center for Cancer/Cancer Hospital, Chinese Academy of Medical Sciences and Peking Union Medical College, Beijing, People's Republic of China, Tel +861087788573, Email lgh0603@cicams.ac.cn

Introduction: Head and neck tumors account for more than 6% of all cancers. The primary treatment for tumors of the head and neck is radiation therapy, which can induce oropharyngeal mucositis as a side effect. At present, there is no widely available therapeutic for the treatment of oropharyngeal mucositis in clinical practice. Based on the traditional prescription Liushen Wan, the pathogenesis and pathology, we developed a new Chinese medicine prescription and made Zhenhuang submicron emulsion (ZHSE) spray, which has an efficacious therapeutic effect for oropharyngeal mucositis. However, its mechanism is unclear.

Methods: This research explored the mechanism behind the modulatory effects of ZHSE by a strategy of metabolomics and network pharmacology. Multivariate data analyses, including unsupervised principal component analysis (PCA) and supervised orthogonal partial least squares discriminant analysis (OPLS-DA), were performed. Potential biomarkers were identified depending on the mass-charge ratio of the selected compound. Statistical and pathway enrichment analysis was performed in the KEGG pathway database. Network pharmacology combining metabolomic analyses was conducted to illustrate the key targets and pathways.

Results: Critical metabolic pathways were investigated, 56f biomarkers were enriched and key metabolites such as linoleic acid, 9, 10-epoxyoctadecenoic acid, acetoacetic acid and citric acid were identified. A complex network of "compound-target-potential metabolite" interactions was drawn to illuminate the regulation of chemical constituents on key metabolites. These findings manifest that ZHSE regulates endogenous metabolite disorders during the treatment of oropharyngeal mucositis by various constituents, interacting with multiple targets associated with inflammation and pain.

Conclusion: In this work, we determined several critical biomarkers and metabolic pathways and identified the possible regulatory mechanism by which ZHSE functions in the treatment of oropharyngeal mucositis. This study provides a new perspective on integrating metabolomics and network pharmacology for exploring improved therapy for head and neck tumors based on the traditional classic prescription of LSW.

Keywords: metabolomics, network pharmacology, mucositis, traditional Chinese medicine, head and neck tumors

Received: 9 June 2022
Accepted: 3 September 2022
Published: 17 September 2022

Introduction

Head and neck tumors generally refer to all malignant tumors from the base of the skull to the clavicle and the front of the cervical spine. They do not include malignant tumors of the skull, cervical spine or eyes. According to the data Global Cancer Statistics 2020, more common head and neck tumors, including tumors located in the thyroid, lip, oral cavity, nasopharynx, oropharynx, and hypopharynx, contributing 1,279,935 new cases and 388,153 deaths, accounting for 6.63% of all cancers (129,927,895 new cases) and 3.90% of all cancer deaths (9,958,133 deaths) worldwide in 2018.[1] The complex anatomical structure and vascular deformation of the head and neck results in poor surgical accessibility. Squamous cell carcinoma, which responds well to radiation therapy, is a common cause of pathological head and neck tumors. Radiotherapy alone or as part of a definitive chemoradiotherapy regimen plays an irreplaceable role in the treatment of head and neck squamous cell carcinoma of different stages.[2]

Radiation-induced mucositis is a common acute side effect during head and neck radiotherapy; it occurs in almost all patients who receive head and neck radiotherapy.[3,4] The clinical symptoms of radiation-induced oropharyngeal mucositis include dry throat, sore throat, foreign body sensation, and trouble swallowing. The extent of the clinical symptoms and duration is related to the field of radiation and the radiation dosage. Radiation therapy can cause infection, inflammation, or other damage to the mucous membrane of the pharynx, resulting in mucosal congestion, redness, ulcers, and gland destruction.

The intense pain caused by radiation-induced mucositis not only affects the intake of nutrients through eating food but can also often require opioid analgesia depending on severity. Mucositis negatively affects the quality of life of head and neck radiotherapy patients.[5] In the case of severe radiation-induced mucositis, suspension of the radiotherapy may be the only course of action, thereby interrupting the chemotherapeutic process,[6] and subsequently impacting treatment efficacy and disease prognosis. Chemotherapy-induced mucositis requires symptomatic treatment and nutritional support and may cause secondary infection and hospitalization.[7] The occurrence of these conditions will result in a heavier economic burden associated with cancer of the head and neck.

At present, there is no widely used drug for the treatment of radiation oropharyngeal mucositis with a recognized effect in clinical practice. Herein, we have formulated a new Chinese medicine formula according to the pathogenesis and pathology based on the traditional classic prescription-Liushen Pill, which we have packaged into a ZHSE spray. ZHSE spray can increase the residence time of the drug at the skin, and at the same time increase the penetration rate of the drug and improve the bioavailability of the drug.

Metabolomics can detect the refined alterations in biological pathways and reveal the profile of the mechanisms that underlie altered physiological processes.[8] Due to the research dilemma caused by the complex components of traditional Chinese medicine and the numerous targets involved, researchers in traditional Chinese medicine have increasingly resorted to metabolomics to explore the mechanism behind its treatment of different diseases.[9] These diseases include but are not limited to coronary heart disease,[10] type 2 diabetes mellitus,[11] metabolic diseases,[12] traumatic brain injury,[13] Alzheimer's disease[14] and lung cancer.[15–17] Network pharmacology is also increasingly applied in the research of traditional Chinese medicine.[18] Abundant information including bioactive compounds, targets, and the interactions between these can be obtained by constructing a network pharmacology model.[19] According to reported data, the paradigm of investigation can be shifted from a "one-target, one-drug" to a "network-target, multiple-component-therapeutics" mode, which is more conducive to the analysis of traditional Chinese medicine.[20]

Preliminary studies have revealed the effectiveness of the preparation of ZHSE. Herein, we conducted a holistic investigation of metabolomics and network pharmacology for profiling the latent mechanism underlying ZHSE in the treatment of oropharyngeal mucositis. Numerous metabolites were identified as being involved in the response to ZHSE in complex biological matrices. Identified metabolites were further applied to the discovery of differentially expressed biomarkers (DEBs) analysis. The related target of DEB, after analysis, was integrated into a multi-path, multi-component, and multi-target network forming a holistic depiction of the mechanism of ZHSE.

Materials and Methods

Chemicals and Reagents HPLC-Grade

Chinese herbal medicine products were purchased from Huamiao Pharmaceutical Co, Ltd. (Beijing, China). ZHSE was self-prepared with decoction products as raw materials. Methanol and Acetonitrile for mobile phases were both HPLC grade; methanol was obtained from Fisher Chemicals (Pittsburgh, PA, United States) and acetonitrile was obtained from Merck (Darmstadt, Germany). Purified water was produced by Millipore's ultrapure water system (Millipore, Bedford, MA, United States). All other chemicals and reagents were of analytical grade and were used as received without further purification unless otherwise indicated.

Preparation of ZHSE

The formula of the ZHSE was derived from the improvement of the classic traditional Liushen pill. The detailed process was represented in a previous study.[21] Briefly, the ZHSE is composed of six raw materials, which meet the requirement of the standards specified by Chinese Pharmacopoeia. Raw materials included MARGARITA, BOVIS CALCULUS ARTIFACTUS, BORNEOLUM SYNTHETICUM, CORYDALIS RHIZOMA, OROXYLI SEMEN and CANARII FRUCTUS at a ratio of 3:3:2:20:20:30. The six raw materials were heated and refluxed with purified water for 1 h. After the extract was concentrated and filtered, the borneol was dissolved in the filtrate as a water extract and 60% ethanol was added and heated at reflux for 1 h. The extract was concentrated and filtered and used as an alcohol extract. An appropriate amount of Tween 80, propylene glycol, lecithin 80H and purified water was added to the water extract, and a high-shear emulsifying and dispersing machine was used to make an aqueous phase. Next, medium-chain triglycerides were added to the alcohol extract and a high-performance dispersing instrument was used to make the oil phase. After mixing the water phase and the oil phase, a high-performance dispersing instrument was utilized to prepare the emulsion. A high-pressure homogenizer was used to homogenize the emulsion to prepare the ZHSE. The micro-emulsion properties utilized were as follows: spherical droplets with a mean diameter of 148.46±5.00nm, a polydispersity index of 0.19±0.04, a zeta potential of −20.11±1.01mv, a marker (with bile acid as a marker) with a concentration of 15.54 ±1.66 μg/mL; the in vitro release of bile acid from 1mL submicron emulsion was 1.22±0.26μg for 60min.

Animals, Oropharyngeal Mucositis Model, and Sample Collection

17 male SD (certificate number 11401300081802) rats at 8 weeks of age, initially weighing 180–220 g, were purchased from Beijing HFK Bioscience Co., Ltd. During the first week of acclimatization, all rats were housed in standard ventilated cages (2–4 per cage) under a constant temperature of 25°C in a 12:12-h light/dark cycle, with free access to standard rat chow and drinking water. The study was approved by the Animal Ethics Committee of Cancer Hospital, Chinese Academy of Medical Sciences. All experimental procedures involving animals complied with the Chinese national legislation and local guidelines.

The modeling methodology was determined according to the results of our previous study regarding oropharynx pathology modeling.[21] In brief, the two groups were modeled using the following method: after the rats were anesthetized and fixed, the rats' tongue was pulled out and pressed down before 15% chloral hydrate was sprayed into its pharynx. This was repeated 3 times a day for 3 days. Animals in the Model group were treated with 3 sprays of distilled water twice per day, once in the morning and afternoon, for 4 days. Meanwhile, animals in the ZHSE group were treated with 3 sprays of ZHSE delivered to the oropharynx once in the morning and afternoon, for 4 days. Animal serum was obtained from blood taken by abdominal aorta after anesthesia 24 hours after the final treatment; the blood was centrifuged and the supernatant was taken after blood coagulation.

Sample Handling for Metabolomics

To a 200 μL sample of serum, 600 μL of methanol was added, and the mixture was mixed by vortexing for 1 min and centrifuged at 10,000 rpm for 10 min at 4 °C. The supernatant obtained after centrifugation was collected and purified with 0.22 μm cellulose syringe filters. A 5-μL aliquot of purified supernatant was analyzed.

Liquid Chromatography and Mass Spectrometry Conditions

Liquid chromatography-mass spectrometry (LC-MS) analysis was performed using a Agilent 6550 iFunnel Q-TOF LC/MS (Agilent Technologies, USA). The chromatographic separations employed a ZORBOX RRHD C18 analytical column (100mm×2.1 mm., 1.7 μm, Agilent Technologies, USA). Binary gradients consisted of ultrapure water with 0.1% formic acid (solvent A) and acetonitrile with 0.1% formic acid (solvent B) with a flow rate of 0.3 mL/min applied for the elution. The gradient program was as follows: Initial 95% A, 0–1 min, 95% A and held for 1 min; 1–9 min, 95 to 60% A; 9–19 min, 60 to 10% A; 19–21 min, 10 to 0% A; 21–25 min, finally 100% B held for 4 min. The total run time was 30 min. The sample injection volume was 4 μL. All samples were maintained at 4°C during the experimental period.

Positive and negative electrospray ionization sources (ESI) were both included with the analysis by Agilent 6550 Q-TOF/MS to profile the entire mass spectrometry. The MassHunter platform (Agilent Technologies, California, United States) was used as is standard to acquire and process the data, with sample products ranging from 80 to 1200 Da. For positive mode and negative mode, typical parameter values were as follows: electrospray capillary voltage 4.0 kV (ESI+) and 3.0 kV (ESI-), nozzle voltage 500 V, nebulizer pressure 45 psig (ESI+) and 35 psig (ESI-), dry gas flow rate 11L/min, dry gas temperature 225 °C (ESI+) and 200°C (ESI-), sheath gas temperature 350°C, sheath gas flow rate 11 L/ min.

Multivariate Data Processing and Identification of Biomarkers

The raw mass spectrum data were standardized by MetaboAnalyst 5.0 (www. metaboanalyst.ca/) to provide a normalized data matrix. Multivariate data analyses, including unsupervised principal component analysis (PCA) and supervised orthogonal partial least squares discriminant analysis (OPLS-DA), were performed using SIMCA-P 14.1 software (Umetrics, Umea, Sweden) to describe the differences and relationships between groups and mine for potential metabolites. S-plots were generated to validate the result by determining whether there was a significant difference based on the position of the variable in the s-plots. Variable contribution of different variables in the OPLS-DA model was depicted by the variable importance in the projection (VIP), and variables with VIP values > 1 were considered to be related to the difference between groups. Meanwhile, variables with the $|p\ (corr)| \geq 0.5$, p-value < 0.05 and folder changes >2 or <0.5 were considered as important molecules for further data analysis. Potential biomarkers were identified in the human metabolome database (http://www.hmdb.ca/) depending on the mass-charge ratio of the selected compound. An online statistical and pathway enrichment analysis was performed in the library of Rattus norvegicus (rat) in the KEGG (www.genome.jp/kegg/) pathway database on the website of MetaboAnalyst 5.0 (http://www.metaboanalyst.ca/).

Exploring Compound-Target-Potential Metabolite Relationships

The relationship between metabolites and their related targets was elucidated using a combination of metabolomics and network pharmacology. All components contained in the six decoction samples used in the preparation of submicron emulsion were obtained from the lab of the systems pharmacology database and analysis website (https://old.tcmsp-e.com/tcmsp.php), while other resources were used to assist in determining the ingredients of medicinal materials. Components with oral bioavailability greater than or equal to 30% and drug-likeness greater than or equal to 0.18 were selected for subsequent analysis;[22] the relevant targets of these medicines were recorded for later integration with metabolite targets. The potential protein targets of the different metabolites were obtained by searching the MBRole 2.0 database (http://csbg.cnb.csic.es/mbrole2/). All data in form of protein ID were converted to their associated UniProt IDs for comparability of results. A "compound-target-metabolite" network was constructed based on the protein-protein interaction (PPI) data and visualized by using. Cytoscape 2.8.3 software (National Institute of General Medical Sciences, United States).

Protein-Protein Interaction Network

Instances of discovery of compounds and metabolites acting together were extracted for key targets and protein interaction analysis. A protein-protein interaction (PPI) network was constructed based on an online analysis of the string database (Version 11.5, https://cn.string-db.org/).

Statistical Analysis

A Kruskal–Wallis H rank-sum test was used to statistically analyze the score results (SPSS version 15.0; IBM: Chicago, IL, USA, 2006). P<0.05 indicated that the differences between groups were statistically significant, and P < 0.01 suggested highly significant differences.

Results

Metabolomics Analysis of Serum

The mass data obtained by high-performance liquid chromatography-mass spectrometry (HPLC-MS) in positive and negative ion modes were entered into a Principal component analysis (PCA) of metabolomic profiles in SIMCA-P 14.1 software to generate a graphical representation and investigate the similarities and differences in principal components between the model group and the ZHSE group. PCA score scatter plots were reported for both ESI + and ESI- mode. The stability of the instrument throughout the analysis process can be verified by the tightness of the distribution of the quality control samples in these graphs (Figure 1). The tightly grouped distribution characteristics of the quality control samples shown indicated that the instrument was stable throughout the analytical process. The variables representing the serum samples of the model group and the ZHSE group were concentrated in different areas of the PCA score scatter plot, indicating that there are significant differences in metabolite levels between the two groups.

To further reveal the potential inter-group variance, the supervised orthogonal partial least squares discriminant analysis (OPLS-DA) model was utilized, as shown in Figure 2. The OPLS-DA scores plot in ESI + and ESI- mode for the model group and the ZHSE group showed clustering in respective regions of the plot, indicating that the model could make accurate predictions in the dimension of the sample groups. Both models are quantitatively described by the parameters R2X (0.792, 0.753) and Q2 (0.914, 0.662) values in the ESI + and ESI- modes, respectively, to illustrate the quality of the model. The characteristics of satisfactory interpretation rate of the matrices with accurate fitness and prediction could be determined by interpreting the value of R2X and Q2 as greater than 0.5.

The S-plots for the model group and the ZHSE group are shown in Figure 3, in which the compounds with a VIP of larger than 1 and p (corr) greater than or equal to 0.5 were marked in red. From the data underlying the S-plots, the variables in red that meet the additional screening criteria (P <0.05 and fold change (FC) > 2 or <0.5) are selected as potential biomarkers for subsequent analysis. According to the classification of molecular ions, A jittered scatter plot (Figure 4) was created to illustrate up- and down-regulated ions with different degrees. An online search in the Human Metabolome Database (https://hmdb.ca/) was conducted to obtain an accurate molecular formula based on the exact mass-to-charge ratio of potential biomarkers.

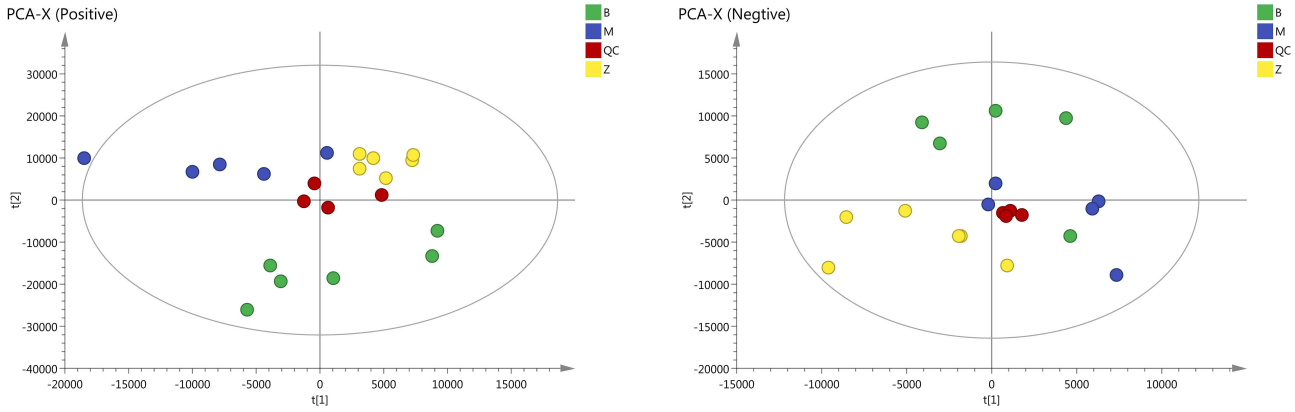

Figure 1 Principal component analysis (PCA) score plots obtained from the quality control group (QC), the blank group (B), the model group (M), and the ZHSE group (Z) in positive and negative electrospray ionization source (ESI) mode.

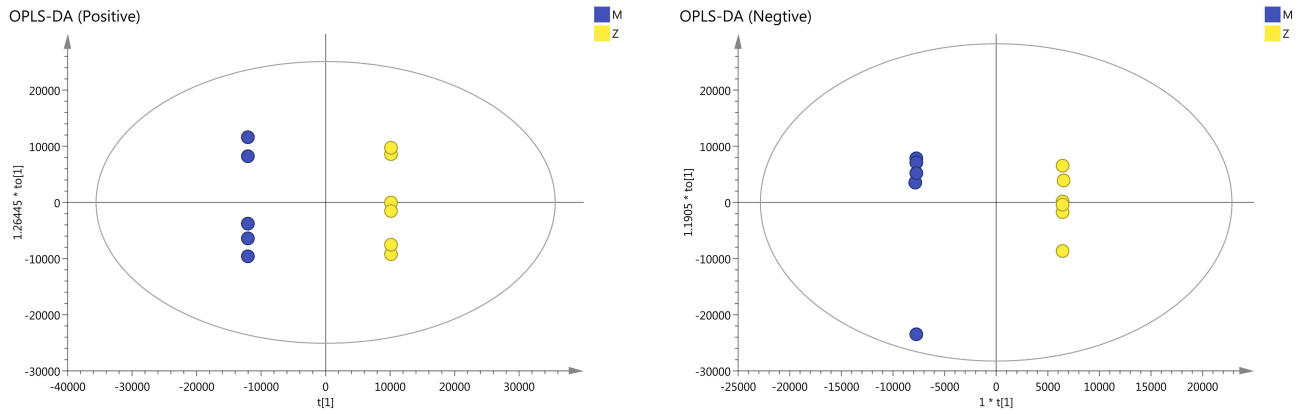

Figure 2 The results of OPLS-DA modeling using the data from the model group (M) and the ZHSE group (Z) in positive and negative electrospray ionization source (ESI) mode.

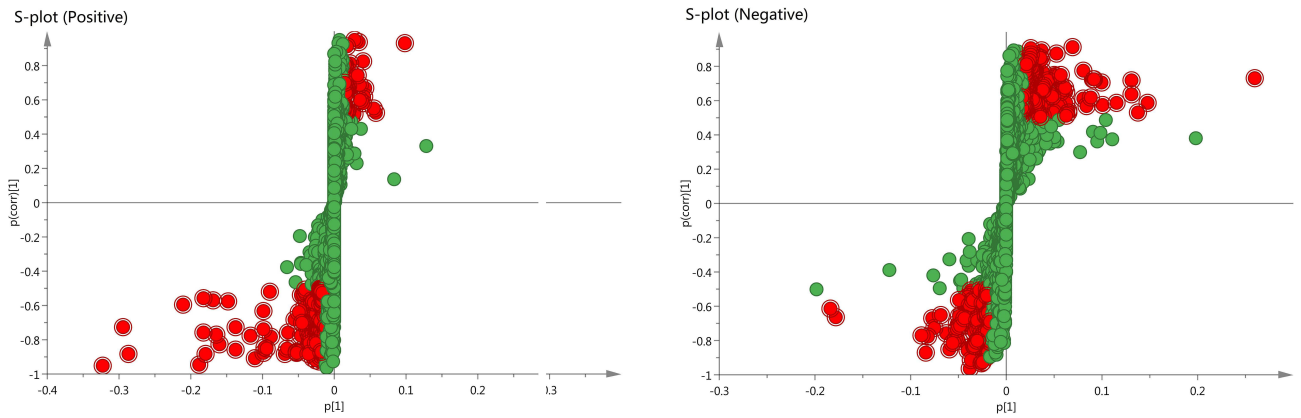

Figure 3 S-score plots constructed from the results in positive and negative modes.

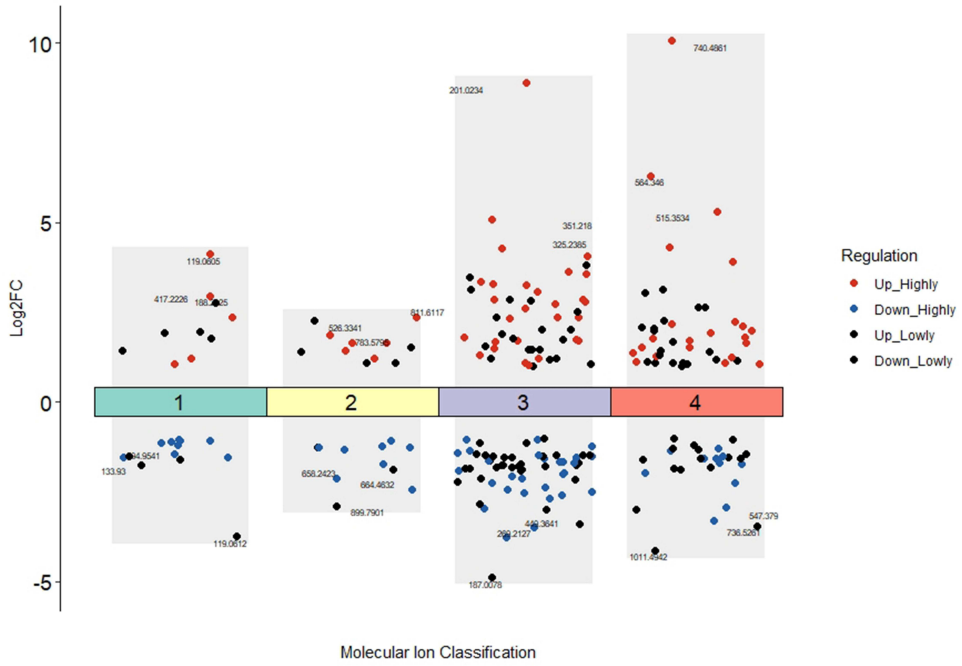

Figure 4 Up- and down-regulated ions with different degrees. The notations are as follows: (1) positive ions with a mass-to-charge ratio greater than 500; (2) positive ions with a mass-to-charge ratio less than 500; (3) negative ions with a mass-to-charge ratio greater than 500; (4) negative ions with a mass-to-charge ratio less than 500.

Identification of Potential Biomarkers and Pathway Enrichment

In total, 161 potential biomarkers were input into the metabolomics data analysis platform, MetaboAnalyst 5.0 for KEGG pathway enrichment. The enrichment analysis bubble diagram is shown in Figure 5, in which parameters such as quantity and p-value are introduced into the Cartesian coordinate system to represent the relationship between the three variables. Fifty-six biomarkers enriched in metabolic pathways were identified. The pathways were allocated high correlations based on a combination of raw p and impact factors, the top 5 of which were linoleic acid metabolism and synthesis, degradation of ketone bodies, the citrate cycle (TCA cycle), arachidonic acid metabolism, in addition to alanine, aspartate, and glutamate metabolism. In these pathways, the metabolites involved include linoleic acid, 9.10-epoxyoctadecenoic acid, acetoacetic acid, citric acid, cis-aconitic acid, 5(S)-hydroperoxyeicosatetraenoic acid, leukotriene A4, prostaglandin E2, and N-acetyl-L-aspartic acid. After the data was normalized by the log2 method, R language was used to draw a clustering heat map (Figure 6), which revealed significant differences in enriched key metabolites between the two groups of samples. A comprehensive network (Figure 7) was created according to the top 5 enriched pathways and the identified potential biomarkers. At the metabolite level, the differences between the model group and the ZHSE group were compared to investigate the mechanism behind the treatment.

"Compound-Target-Potential Metabolite" Network Construction Based on Network Pharmacology

According to search results from the TCMSP website, we obtained a total of 104 non-repetitive compounds (Supplementary Table 1) and 315 non-repetitive targets related to them. Considering the targets associated with chemical constituents of the drug, as well as the potential metabolites screened in the above experiment, we drew a diagram of the complex network of the "compound-target-potential metabolite" interactions, to identify the regulatory effects that chemical constituents of ZHSE have on metabolites. As shown in Figure 8, 96 active chemical constituents, 277 targets linked to them, 41 potential metabolites, and 488 targets related to potential metabolites contributed to the interactive "potential metabolite-target-component" network.

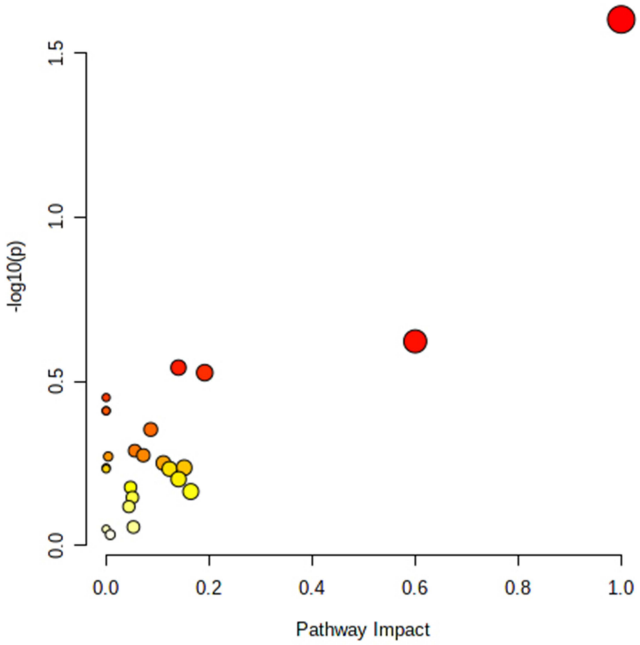

Figure 5 The bubble diagram from the enrichment analysis.

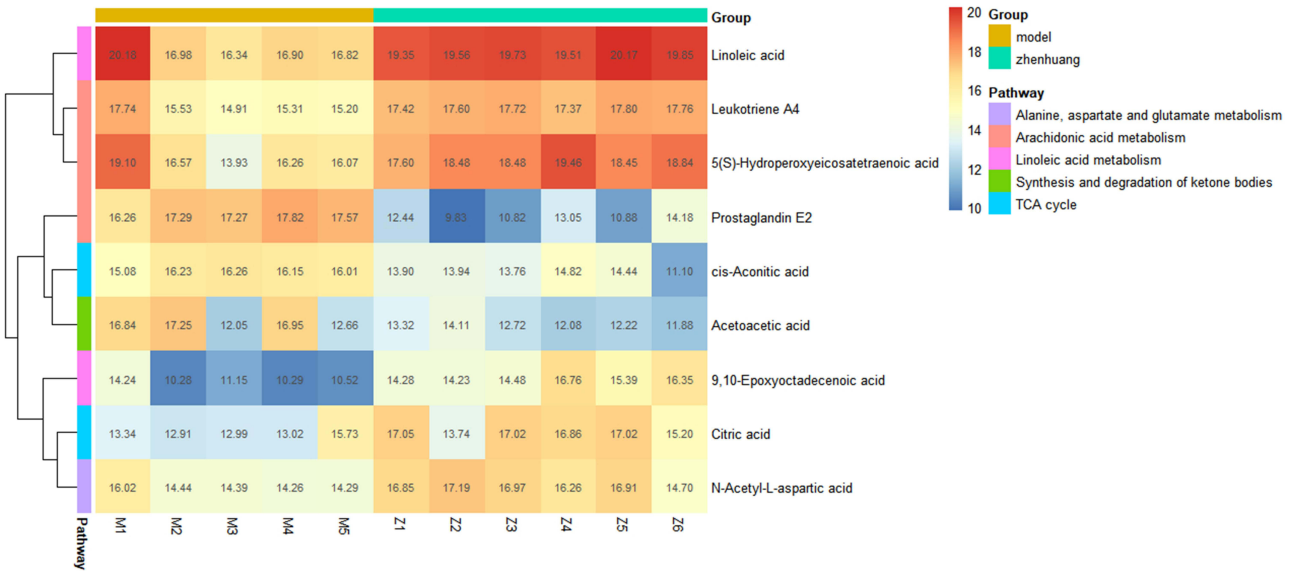

Figure 6 The clustering heatmap of the enriched key differential metabolites in different samples.

"Protein-Protein-Interaction" Network Construction

51 proteins co-targeted by compounds and metabolites were searched from the "Potential Metabolite-Target-Component" interaction network. According to analysis results from the STRING website, a total of 50 non-repetitive items with interactions were introduced into the protein-protein interaction network (Figure 9).

Discussion

Liu Shen Wan (LSW) is a classic prescription with hundreds of years of history in traditional Chinese medicine. This prescription contains six medicinal materials including bezoar, toad venom, musk, pearl powder, borneol, and realgar.[23,24] Based on its detoxification and anti-inflammatory pharmacological effect, it is widely used in the treatment of many inflammatory throat diseases including influenza, tonsillitis, pharyngitis, mumps, etc.[24] According to the theory of traditional Chinese medicine, the research presented herein prepared ZHSE spray by recombining the prescription and using modern technology. The results of previous studies revealed that ZHSE was more effective than LSW after prescription adjustment. It could significantly reduce the inflammatory lesions in rats with acute pharyngitis without any toxic side effects and was also shown to inhibit the expression of many inflammatory-related factors in the serum of model animals.[21]

To further clarify the mechanism of ZHSE, we studied the correlation between metabolomic characteristics and the phenotypic characteristics of oropharyngeal mucositis. In this study, 56 differentially expressed metabolites were identified, which were enriched in 22 metabolic pathways (Figure 4). Linoleic acid metabolism and synthesis, degradation of ketone bodies, the citrate cycle (TCA cycle), arachidonic acid metabolism, and alanine, aspartate, and glutamate metabolism were the main pathways that were enriched.

ZHSE appears to play a major role in inflammatory development and pain regulation through the linoleic acid metabolism and synthesis pathways. Oxidized linoleic acid metabolites may be important targets for reducing mechanical and thermal hyperalgesia in peripheral inflammation from acute to chronic causes of inflammation and inflammatory pain.[25] In terms of pain, both low oleic acid intake[26,27] in clinical trials and decreases in oleic acid levels in blood[28] showed strong correlations with pain reduction, indicating oleic acid and its derivatives were an influential family of endogenous mediators that mediate chronic pain and itchiness.[29] In terms of inflammation, Cytochrome P450-derived linoleic acid metabolites, NF-κB, and AP-1 transcription factors all mediate inflammation and could be activated by linoleic acid and high concentrations of 9.10-EpOME and 9.10-DiHOME. However, another oleic acid derivative, 12.13-

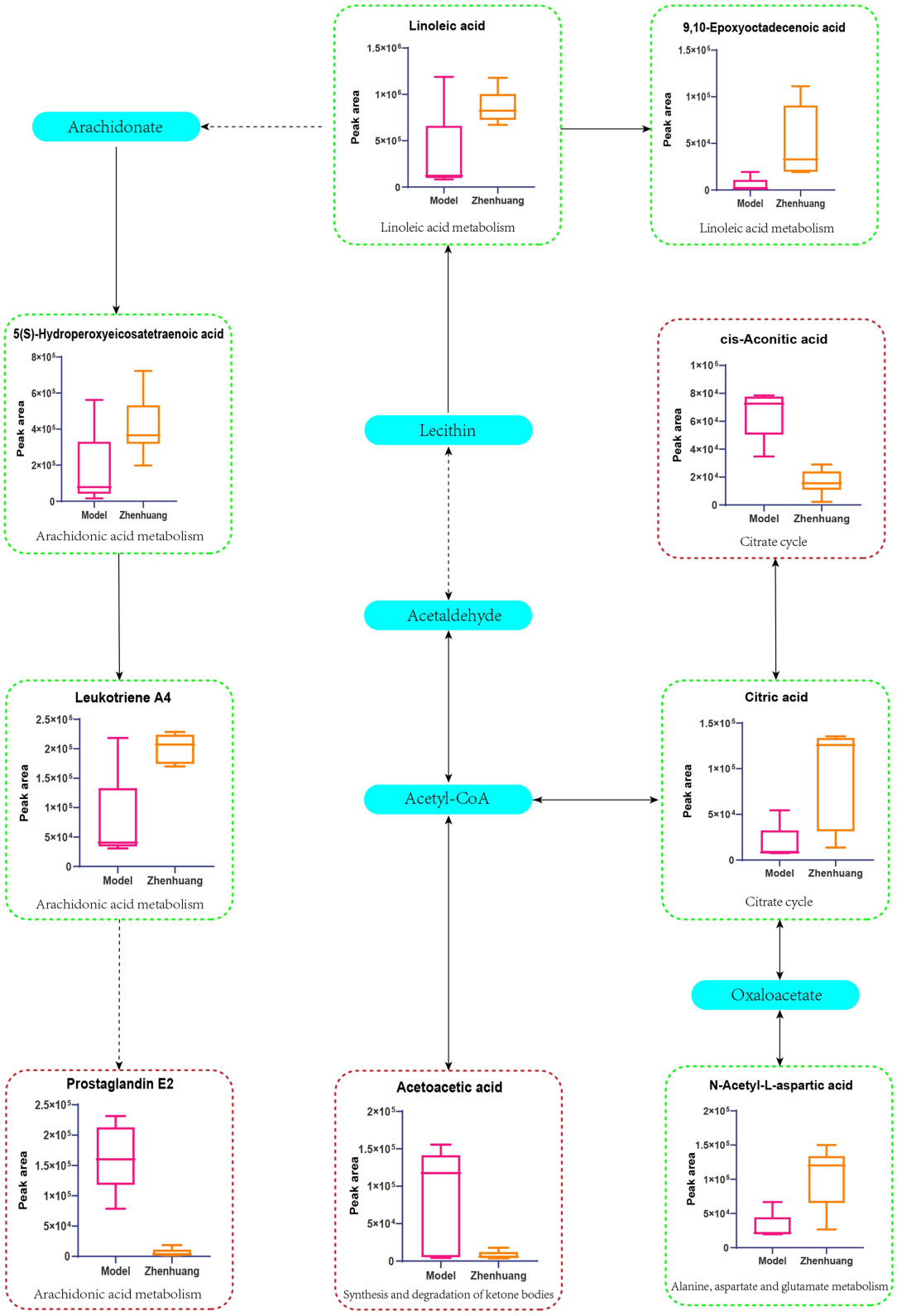

Figure 7 Schematic diagram of the metabolic pathways related to ZHSE and the trends of biomarkers enriched in these metabolic pathways. The notations are as follows: (↑) in green boxes, metabolite higher in the ZHSE group than in the model group; (↓) in red boxes, metabolite lower in the ZHSE group than in the model group. The relevant metabolic pathways are described at the bottom of the boxes.

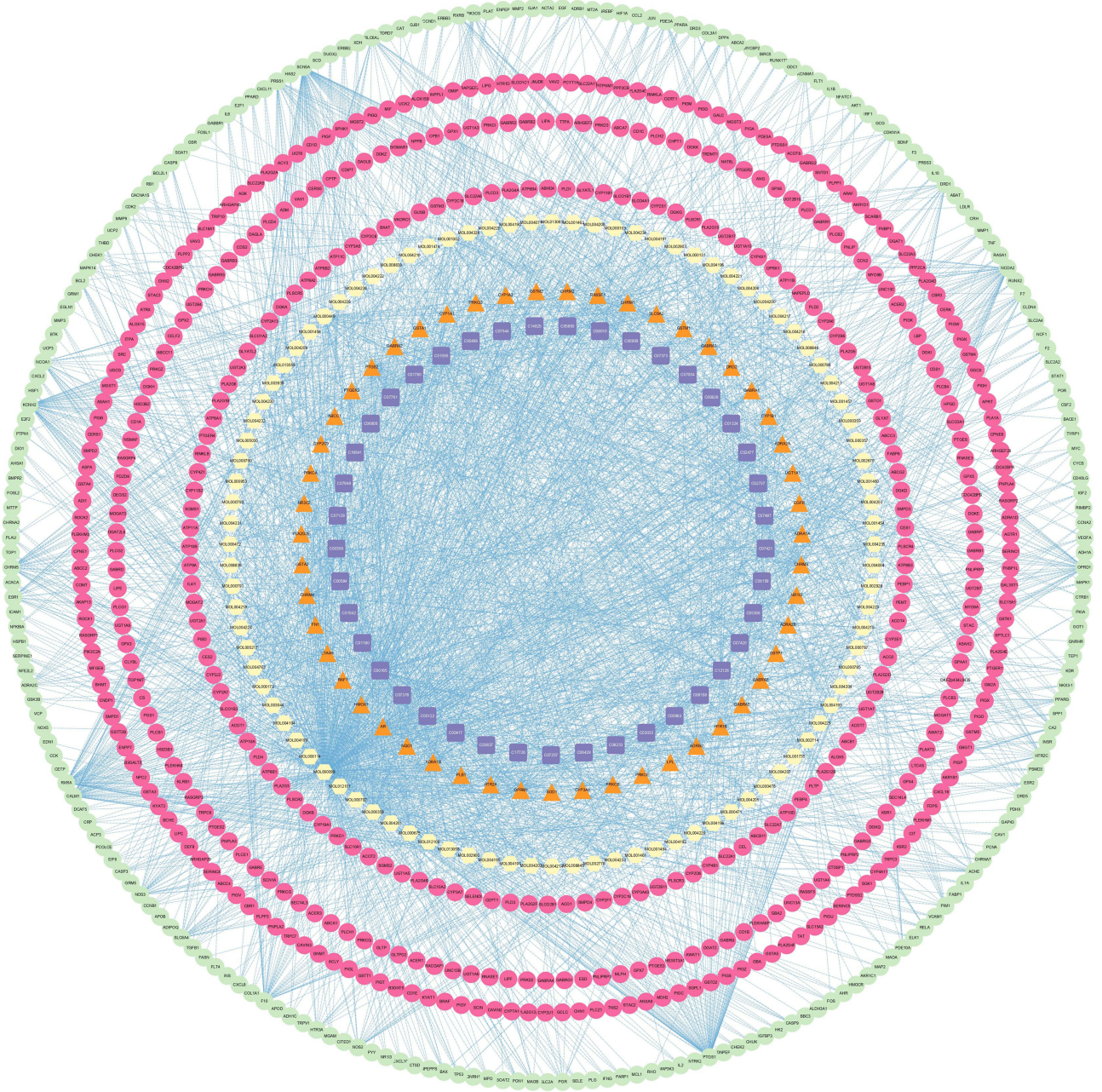

Figure 8 The "Potential Metabolite-Target-Component" interaction network with all target information for active chemical constituents and potential metabolites. The yellow nodes represent active chemical constituents of the ZHSE. The purple nodes represent potential metabolites. The green nodes represent the protein targets of active chemical constituents. The pink nodes represent the targets associated with potential metabolites. The orange nodes represent the proteins that were targets of both active chemical constituents and potential metabolites.

DiHOME may contribute to the suppression of the immune response, as evidenced by its ability to inhibit the respiratory burst and its increase in concentrations in healthy adult men during intralipid infusion.[30] The levels of Linoleic acid and 9.10-Epoxyoctadecenoic acid in the ZHSE group were significantly increased compared with the model group, which suggested that ZHSE might accelerate the body's natural immune response and inflammatory response process by inducing NF-κB and AP-1 transcription factors to treat oropharyngeal mucositis. Moreover, the consumption of oleic acid and its derivatives at this stage also helps to avoid the conversion of acute oropharyngeal mucositis to chronic oropharyngeal mucositis and inhibit the associated pain.

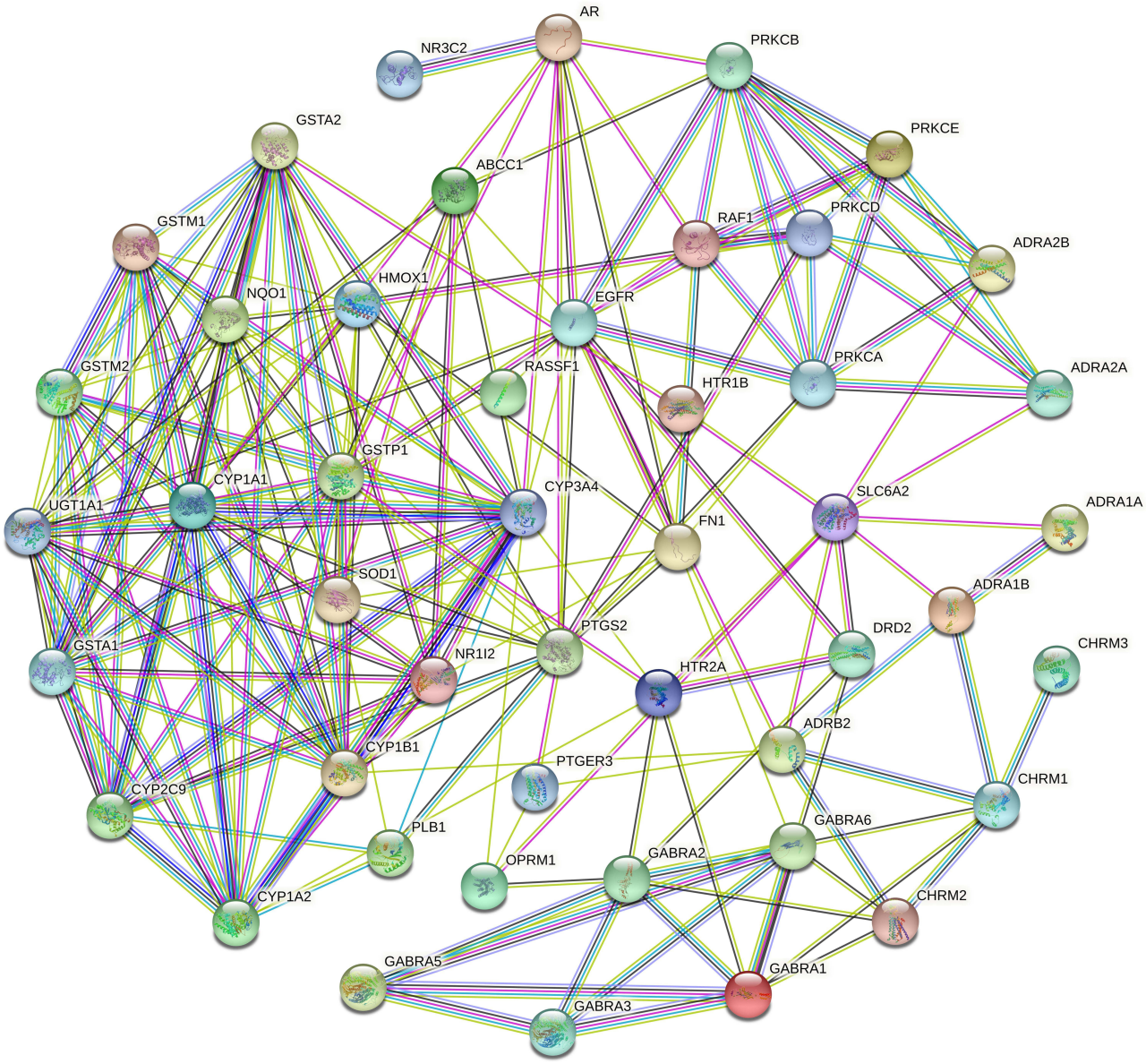

Figure 9 The "Protein-protein-interaction" network with target proteins co-targeted by compounds and metabolites. Purple edges: known Interactions (from curated databases). Pink edges: known Interactions (experimentally determined). Green, red and blue edges: Predicted Interactions.

The arachidonic acid metabolism pathway is another substantial metabolic pathway identified in the enrichment analysis that serves as an inflammatory regulatory pathway for the treatment of oropharyngeal mucositis. Arachidonic acid generation is initiated by cyclooxygenase and lipoxygenases and is used in two complex biochemical cascade reactions to generate prostaglandins, prostacyclins, thromboxanes (catalyzed by cyclooxygenase) and leukotrienes (catalyzed by lipoxygenases).[31] There is a complex synergistic network of biochemical factors involved in the process of inflammation, in which arachidonic acid and its metabolites, together with mediators released by activating other inflammatory cells, form the nodes of the cooperative network. The cooperation of mediators varies according to the inflammatory situation and anatomical location.[31] As shown in Figure 5, due to the action of ZHSE, 5(S)-Hydroperoxyeicosatetraenoic acid and leukotriene A4 are up-regulated, and prostaglandin E2 is down-regulated; these metabolic variations allow the modulation of the immune network to further improve the treatment process for pharyngitis. LTA4 can be further modified to LTB4,[32] which is involved in the initiation and regulation of immune response and M1 macrophage potentiation.[33] Prostaglandin E2 (PGE2) facilitates the generation of

M1.[33] EP4-receptor-mediated downregulation of PGE2 was observed in human systemic inflammation disease.[34] Arachidonic acid (AA) metabolism plays a critical role in initiating and regulating inflammation.[33]

After integrating the data regarding the drug components in Chinese Herbal Medicines and the post-administration differential metabolites, 51 common targets were obtained through network pharmacology analysis, suggesting that these targets may be of great significance for treating the radiation oropharyngeal mucositis and uncovering the underlying mechanism.

Among the many common targets, some were related to inflammation, and these targets may affect the regulation of inflammation in radiation oropharyngeal mucositis. LTB4 is a potent pro-inflammatory lipid mediator, with a large body of scientific literature describing its diverse roles in inflammatory processes. The catalytic activity of leukotriene A4 hydrolase (LTA4H) plays an important role in inflammatory processes; it has two distinct but overlapping active sites that confer different catalytic activities.[35] LTB4 is involved in inducing anti-microbial factors, the release of inflammatory mediators, enhancing phagocytosis, and is also implicated in diseases in which neutrophils are strongly involved.[36] In allergic mucosal inflammation, LTB4 expression levels are significantly increased in Neutrophils, monocytes, and lymphocytes, suggesting a strong involvement in this process.[37] Some studies have confirmed that the expression of PRKCA is closely related to the inflammatory response of different systems, including the respiratory system and digestive system. It has been reported that acute lung injury and associated inflammatory responses could be alleviated by promoting the expression of PRKCA,[38] and esophageal inflammation development was linked to elevating the expression of PRKCA.[39] There may therefore be some indirect effect of inflammatory inducers of NF-κB that not only could activate inflammation, but also could alter the regulation of gene expression of PRKCA.[40]

In the treatment of oropharyngeal mucositis with ZHSE, which upstream pathways are incorporated to regulate metabolism and the key target protein? After the general direction of the interaction of the various chemical components from the ZHSE was clarified, by which mechanism do they work exactly during oropharyngeal mucositis treatment? Answering these questions will require further research and elucidation. In conclusion, these findings manifest that ZHSE regulates endogenous metabolite disorders during the treatment of oropharyngeal mucositis by various constituents interacting with multiple targets linked to inflammation and pain. This study provides a new perspective on integrating metabolomics and network pharmacology for exploring the improved treatment based on the traditional classic prescription of LSW.

Abbreviations

AA, arachidonic acid; DEBs, differentially expressed biomarkers; ESI, electrospray ionization; FC, fold change; HPLC-MS, high-performance liquid chromatography-mass spectrometry; LC-MS, liquid chromatography-mass spectrometry; LSW, Liu Shen Wan; LTA4H, leukotriene A4 hydrolase; LTB4, leukotriene B4; OPLS-DA, orthogonal partial least squares discriminant analysis; PCA, principal component analysis; PGE2, prostaglandin E2; PPI, protein-protein interaction; TCA cycle, the citrate cycle; VIP, variable importance in the projection; ZHSE, Zhenhuang submicron emulsion.

Data Sharing Statement

The data supporting the conclusions of this article will be made available by the corresponding author upon request, without undue reservation.

Acknowledgments

This work was supported by Beijing Hope Run Special Fund of Cancer Foundation of China (grants No. LC2020A27).

Disclosure

The authors declare that the research was conducted in the absence of any commercial or financial relationships that could be construed as a potential conflict of interest.

References

1. Sung H, Ferlay J, Siegel RL, et al. Global cancer statistics 2020: GLOBOCAN estimates of incidence and mortality worldwide for 36 cancers in 185 countries. *CA Cancer J Clin*. 2021;71(3):209–249. doi:10.3322/caac.21660
2. Snow GB. Head and neck cancer. *Curr Opin Oncol*. 1992;4(3):469–470. doi:10.1097/00001622-199206000-00007
3. Maria OM, Eliopoulos N, Muanza T. Radiation-induced oral mucositis. *Front Oncol*. 2017;7. doi:10.3389/fonc.2017.00089

4. Elad S, Cheng KKF, Lalla RV, et al. MASCC/ISOO clinical practice guidelines for the management of mucositis secondary to cancer therapy. *Cancer*. 2020;126(19):4423–4431. doi:10.1002/cncr.33100
5. Kusiak A, Alicjajereczek-Fossa B, Cichońska D, Alterio D. Oncological-therapy related oral mucositis as an interdisciplinary problem—literature review. *Int J Environ Res Public Health*. 2020;17(7):2464. doi:10.3390/ijerph17072464
6. Co JL, Mejia MBA, Que JC, Dizon JMR, Eisele DW. Effectiveness of honey on radiation-induced oral mucositis, time to mucositis, weight loss, and treatment interruptions among patients with head and neck malignancies: a meta-analysis and systematic review of literature. *Head Neck*. 2016;38(7):1119–1128. doi:10.1002/hed.24431
7. Elting LS, Cooksley C, Chambers M, Cantor SB, Manzullo E, Rubenstein EB. The burdens of cancer therapy. *Cancer*. 2003;98(7):1531–1539. doi:10.1002/cncr.11671
8. Johnson CH, Ivanisevic J, Siuzdak G. Metabolomics: beyond biomarkers and towards mechanisms. *Nat Rev Mol Cell Biol*. 2016;17(7):451–459. doi:10.1038/nrm.2016.25
9. Wang M, Chen L, Liu D, Chen H, Tang DD, Zhao YY. Metabolomics highlights pharmacological bioactivity and biochemical mechanism of traditional Chinese medicine. *Chem Biol Interact*. 2017;273:133–141. doi:10.1016/j.cbi.2017.06.011
10. Gao-Song W, Hou-Kai L, Zhang WD. Metabolomics and its application in the treatment of coronary heart disease with traditional Chinese medicine. *Chin J Nat Med*. 2019;17(5):321–330. doi:10.1016/S1875-5364(19)30037-8
11. Pan L, Li Z, Wang Y, Zhang B, Liu G, Liu J. Network pharmacology and metabolomics study on the intervention of traditional Chinese medicine Huanglian Decoction in rats with type 2 diabetes mellitus. *J Ethnopharmacol*. 2020;258:112842. doi:10.1016/j.jep.2020.112842
12. Wu G, Zhang W, Li H. Application of metabolomics for unveiling the therapeutic role of traditional Chinese medicine in metabolic diseases. *J Ethnopharmacol*. 2019;242(1200):112057. doi:10.1016/j.jep.2019.112057
13. Xia Z, Liu W, Zheng F, et al. VISSA-PLS-DA-based metabolomics reveals a multitargeted mechanism of traditional Chinese medicine for traumatic brain injury. *ASN Neuro*. 2020;12:175909142091095. doi:10.1177/1759091420910957
14. Zhang Z, Yi P, Yang J, et al. Integrated network pharmacology analysis and serum metabolomics to reveal the cognitive improvement effect of Bushen Tiansui formula on Alzheimer's disease. *J Ethnopharmacol*. 2020;249(139):112371. doi:10.1016/j.jep.2019.112371
15. Li C, Chen W, Zhang M, et al. Modulatory effects of Xihuang Pill on lung cancer treatment by an integrative approach. *Biomed Pharmacother*. 2020;130:110533. doi:10.1016/j.biopha.2020.110533
16. Li C, Niu M, Wang R, et al. The modulatory properties of Si Jun Zi Tang enhancing anticancer of gefitinib by an integrating approach. *Biomed Pharmacother*. 2019;111(17):1132–1140. doi:10.1016/j.biopha.2018.12.026
17. Li C, Wang Z, Chen W, et al. An integrative metabolomic and network pharmacology study revealing the regulating properties of Xihuang pill that improves anlotinib effects in lung cancer. *Front Oncol*. 2021;11:1–14. doi:10.3389/fonc.2021.697247
18. Luo TT, Lu Y, Yan SK, Xiao X, Rong XL, Guo J. Network pharmacology in research of Chinese medicine formula: methodology, application and prospective. *Chin J Integr Med*. 2020;26(1):72–80. doi:10.1007/s11655-019-3064-0
19. Li S, Zhang B. Traditional Chinese medicine network pharmacology: theory, methodology and application. *Chin J Nat Med*. 2013;11(2):110–120. doi:10.1016/S1875-5364(13)60037-0
20. Zhang R, Zhu X, Bai H, Ning K. Network pharmacology databases for traditional Chinese medicine: review and assessment. *Front Pharmacol*. 2019;10:1–14. doi:10.3389/fphar.2019.00123
21. Qi S, Shi Y, Feng X, et al. Effect of Zhenhuang Submicron Emulsion on acute pharyngitis model rats. *World J Integr Tradit West Med*. 2020;15(3):7–10.
22. Chen J, Wang YK, Gao Y, Hu LS, Yang JW, Wang JR. Protection against COVID-19 injury by qingfei paidu decoction via anti- viral, anti-inflammatory activity and metabolic programming. *Biomed Pharmacother*. 2020;129:1–16. doi:10.1016/j.biopha.2020.110281
23. Wang J, Ding L, Zhou J, et al. Target lipidomics approach to reveal the resolution of inflammation induced by Chinese medicine combination in Liu-Shen-Wan against realgar overexposure to rats. *J Ethnopharmacol*. 2020;249:112171. doi:10.1016/j.jep.2019.112171
24. Zhao J, Wang Y, Huang X, et al. Liu Shen Wan inhibits influenza virus-induced secondary Staphylococcus aureus infection in vivo and in vitro. *J Ethnopharmacol*. 2021;277:114066. doi:10.1016/j.jep.2021.114066
25. Wedel S, Osthues T, Zimmer B, Angioni C, Geisslinger G, Sisignano M. Oxidized linoleic acid metabolites maintain mechanical and thermal hypersensitivity during sub-chronic inflammatory pain. *Biochem Pharmacol*. 2022;198:114953. doi:10.1016/j.bcp.2022.114953
26. Ramsdena CE, Faurot KR, Zamora D, et al. Targeted alteration of dietary n-3 and n-6 fatty acids for the treatment of chronic headaches: a randomized trial. *Pain*. 2013;154:2441–2451. doi:10.1016/j.earlhumdev.2006.05.022
27. Ramsden CE, Faurot KR, Zamora D, et al. Targeted alterations in dietary n-3 and n-6 fatty acids improve life functioning and reduce psychological distress among chronic headache patients: secondary analysis of a randomized trial. *Pain*. 2015;156:587–596. doi:10.1097/01.j.pain.0000460348.84965.47.Targeted
28. Ramsden CE, Zamora D, Makriyannis A. Diet-induced changes in n-3 and n-6 derived endocannabinoids and reductions in headache pain and psychological distress. *J Pain*. 2015;16:707–716. doi:10.1530/ERC-14-0411
29. Ramsden CE, Domenichiello AF, Yuan ZX, et al. A systems approach for discovering linoleic acid derivatives that potentially mediate pain and itch. *Sci Signal*. 2018;10(62):1–24. doi:10.1126/scisignal.aal5241.A
30. Kelsey Hildreth SD, Kodani BD, Hammock LZ. Cytochrome P450-derived linoleic acid metabolites EpOMEs and DiHOMEs: a review of recent studies. *J Nutr Biochem*. 2020;86:1–22. doi:10.1016/j.jnutbio.2020.108484.Cytochrome
31. Zenner HP, Brunner FX. Immunological aspects of tonsils and of tonsillitis. *Acta Otolaryngol*. 1988;105(S454):70–74. doi:10.3109/00016488809125008
32. Gilbert NC, Newcomer ME, Werz O. Untangling the web of 5-lipoxygenase-derived products from a molecular and structural perspective: the battle between pro- and anti-inflammatory lipid mediators. *Biochem Pharmacol*. 2021;193:114759. doi:10.1016/j.bcp.2021.114759
33. Das UN. Essential fatty acids and their metabolites in the pathobiology of inflammation and its resolution. *Biomolecules*. 2021;11(12):1873. doi:10.3390/biom11121873
34. Duffin R, O'Connor RA, Crittenden S, et al. Prostaglandin E2 constrains systemic inflammation through an innate lymphoid cell-IL-22 axis. *Science*. 2016;351(6279):1333–1338. doi:10.1126/science.aad9903
35. Teixeira CSS, Sousa SF. Current status of the use of multifunctional enzymes as anti-cancer drug targets. *Pharmaceutics*. 2022;14(1):1–25. doi:10.3390/pharmaceutics14010010

36. Röhn TA, Numao S, Otto H, Loesche C, Thoma G. Drug discovery strategies for novel leukotriene A4 hydrolase inhibitors. *Expert Opin Drug Discov*. 2021;16(12):1483–1495. doi:10.1080/17460441.2021.1948998
37. Plewako H, Holmberg K, Oancea I, Rak S. Increased expression of lipoxygenase enzymes during pollen season in nasal biopsies of pollen-allergic patients. *Allergy*. 2006;61(6):725–730. doi:10.1111/j.1398-9995.2006.00980.x
38. Wang M, Zhong H, Zhang X, et al. EGCG promotes PRKCA expression to alleviate LPS-induced acute lung injury and inflammatory response. *Sci Rep*. 2021;11(1):1–12. doi:10.1038/s41598-021-90398-x
39. Guo Y, Bao Y, Ma M, et al. Clinical significance of the correlation between PLCE 1 and PRKCA in esophageal inflammation and esophageal carcinoma. *Oncotarget*. 2017;8(20):33285–33299. doi:10.18632/oncotarget.16635
40. Stoney PN, Rodrigues D, Helfer G, et al. A seasonal switch in histone deacetylase gene expression in the hypothalamus and their capacity to modulate nuclear signaling pathways. *Brain Behav Immun*. 2017;61:340–352. doi:10.1016/j.bbi.2016.12.013